Shear-wave traveltimes in inhomogeneous weakly anisotropic media

Einar Iversen, NORSAR, Véronique Farra, Institut de Physique du Globe de Paris, and Ivan Pšenčík, Institute of Geophysics, Acad. Sci. of Czech Republic*

Summary

A useful byproduct of studying shear-wave coupling in inhomogeneous weakly anisotropic media are formulae for approximate evaluation of traveltimes of separate S waves. The traveltimes can be obtained from perturbations computed along so-called first-order S-wave common rays. The perturbations consist of two parts. The first represents correction of the traveltime computed along the first-order common ray. The other controls separation of S waves. Both parts can be simply evaluated by quadratures along the common ray. The formulae have applications in migration and traveltime tomography.

Introduction

S waves propagating in inhomogeneous, weakly anisotropic media are usually coupled. Coupling is well described by the coupling ray theory (Coates and Chapman, 1990; Bulant and Klimeš, 2002). Important role in the coupling ray theory is played by the trajectory - common S-wave ray - along which coupling effects are evaluated. To construct such a common ray, Bakker (2002) proposed the use of an artificial Hamiltonian obtained as the average of the actual Hamiltonians of the two S waves propagating in an anisotropic medium, see also Klimeš (2006). Farra and Pšenčík (2008, 2009) used Bakker's (2002) approach and combined it with the first-order ray tracing (FORT) and first-order dynamic ray tracing (FODRT) concepts (Pšenčík and Farra, 2005, 2007), which they used earlier for computing P waves in inhomogeneous weakly anisotropic media.

Farra and Pšenčík (2009) show that the S-wave common ray concept used in the coupling ray theory can be also used for the approximate evaluation of traveltimes of separate S waves propagating in inhomogeneous weakly anisotropic media. Such traveltime estimates are of particular interest for migration and tomography applications. Here we present basic formulae obtained by Farra and Pšenčík (2009) and illustrate their accuracy in numerical tests.

The lower-case indices $i,j,k,l,...$ take the values of 1,2,3, the upper-case indices $I,J,K,L,...$ take the values of 1,2. The Einstein summation convention over repeated indices is used. The upper index $[\mathscr{M}]$ is used to denote quantities related to the S-wave common ray.

Theory

The first-order common S-wave ray in an inhomogeneous weakly anisotropic medium can be obtained by solving the first order ray tracing (FORT) equations

$$\frac{dx_i}{d\tau}=\frac{1}{2}\frac{\partial G^{[\mathscr{M}]}(x_m,p_m)}{\partial p_i},\qquad \frac{dp_i}{d\tau}=-\frac{1}{2}\frac{\partial G^{[\mathscr{M}]}(x_m,p_m)}{\partial x_i}. \tag{1}$$

Here x_i and p_i are the Cartesian coordinates of the S-wave common first-order ray and the components of the corresponding first-order slowness vectors, respectively. Parameter $\tau=\tau^{[\mathscr{M}]}(x_m)$ is the first-order traveltime calculated along the common ray. Symbol $G^{[\mathscr{M}]}$ denotes the first-order S-wave mean eigenvalue

$$G^{[\mathscr{M}]}(x_m,p_m)=\tfrac{1}{2}(G^{[1]}+G^{[2]}). \tag{2}$$

In equation 2, $G^{[1]}$ and $G^{[2]}$ are the first-order approximations of two smaller eigenvalues of the generalized Christoffel matrix Γ:

$$\Gamma_{ik}(x_m,p_m)=a_{ijkl}(x_m)p_jp_l\ . \tag{3}$$

Symbols a_{ijkl} denote density-normalized elastic moduli,

$$a_{ijkl}=c_{ijkl}/\rho\ , \tag{4}$$

c_{ijkl} being elements of the fourth-order tensor of elastic moduli and ρ the density.

Farra and Pšenčík (2009) show that the common ray and traveltime $\tau^{[\mathscr{M}]}(\tau,\tau_0)$ calculated along it between points corresponding to τ_0 and τ on the common S-wave ray can be used for approximate determination of traveltimes of separate S waves. Assuming that the common S-wave ray does not pass through a singularity, we can write the expressions for the approximate traveltimes τ_{S1} and τ_{S2} of faster S1 and slower S2 waves between points corresponding to τ_0 and τ on the common S-wave ray as:

$$\tau_{S1,S2}(\tau,\tau_0)=\tau^{[\mathscr{M}]}(\tau,\tau_0)+\Delta\tau_{S1,S2}(\tau,\tau_0)\ . \tag{5}$$

The term $\tau^{[\mathscr{M}]}(\tau,\tau_0)$ is the first-order traveltime, the perturbation $\Delta\tau_{S1,S2}$ is given by the following formula:

$$\Delta\tau_{S1}=\Delta\tau^{[\mathscr{M}]}-\frac{1}{4}\int_{\tau_0}^{\tau}\sqrt{(M_{11}-M_{22})^2+4M_{12}^2}\,d\tau,$$
$$\Delta\tau_{S2}=\Delta\tau^{[\mathscr{M}]}+\frac{1}{4}\int_{\tau_0}^{\tau}\sqrt{(M_{11}-M_{22})^2+4M_{12}^2}\,d\tau. \tag{6}$$

The term $\Delta\tau^{[\mathscr{M}]}$ in equation 6 is the second-order correction of the traveltime along the common S-wave ray, the second terms on the right-hand sides control separation of S waves.

The second-order traveltime correction $\Delta\tau^{[\mathscr{M}]}$ is given by the formula:

$$\Delta\tau^{[\mathscr{M}]}=\frac{1}{4}\int_{\tau_0}^{\tau}[c^{[\mathscr{M}]}(x_m,n_m)]^2\frac{B_{13}^2(x_m,p_m)+B_{23}^2(x_m,p_m)}{V_P^2(x_m)-V_S^2(x_m)}d\tau. \tag{7}$$

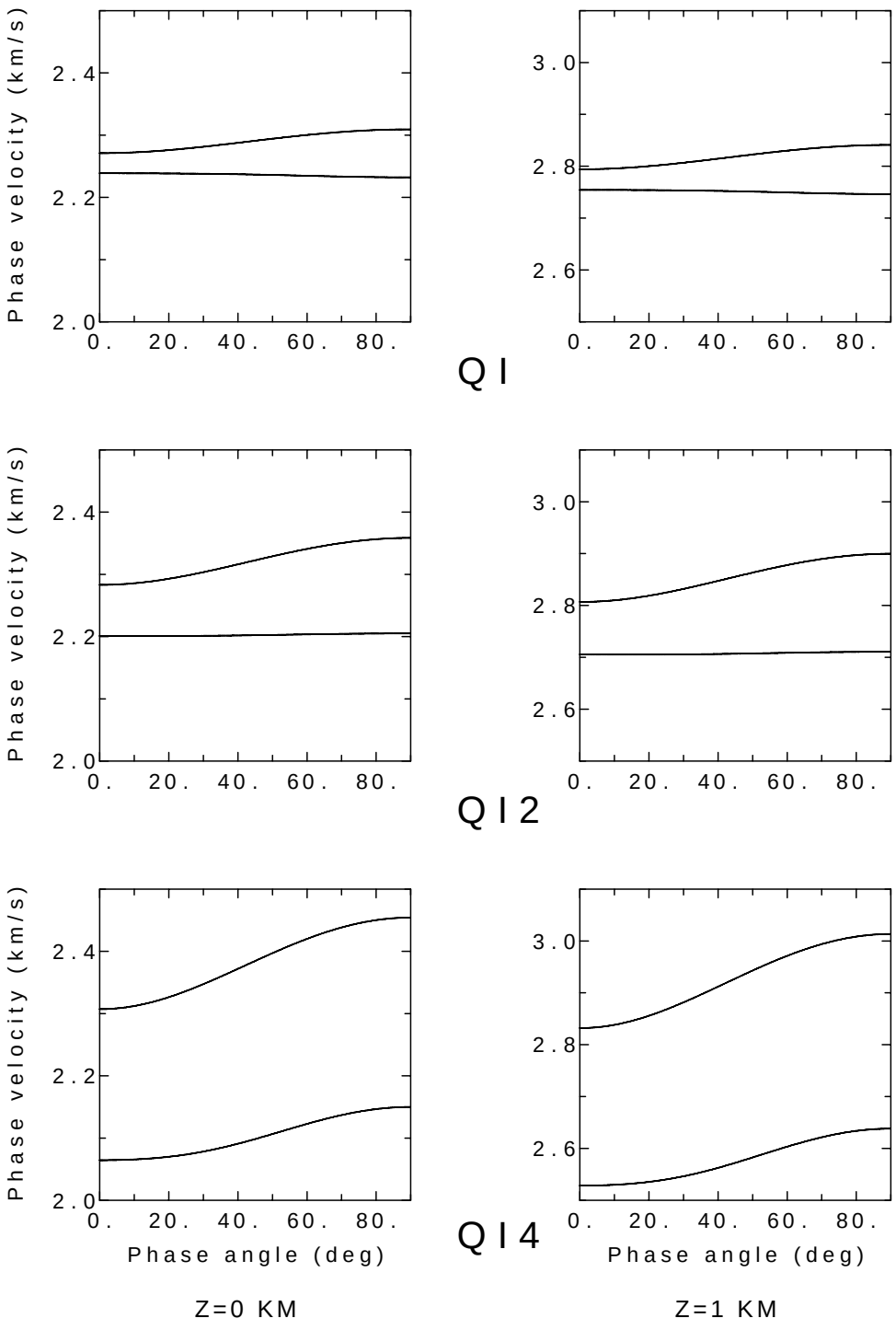

Figure 1: The S-wave phase-velocity sections in the (x,z) plane for models QI (top), QI2 (middle) and QI4 (bottom). The velocities vary from the horizontal (0^0) to vertical (90^0) direction of the wave normal. Left-hand plots correspond to $z = 0$ km, right-hand plots to $z = 1$ km.

The symbols V_S and V_P denote the S- and P-wave velocities of the reference isotropic medium, and they are chosen in the following specific and unique way,

$$V_S^2(x_m) = (c^{[\mathscr{M}]})^2 \ , \quad V_P^2(x_m) = (c^{[\mathscr{M}]})^2 B_{33}(x_m, p_m). \quad (8)$$

Here, $c^{[\mathscr{M}]}$ is the first-order S-wave common phase velocity corresponding to $G^{[\mathscr{M}]}$, $(c^{[\mathscr{M}]})^2(x_m, n_m) = G^{[\mathscr{M}]}(x_m, n_m)$. Quantities B_{ij} in eq. 7 and 8 are elements of the symmetric matrix $\mathbf{B}(x_m, p_m)$:

$$B_{jl}(x_m, p_m) = \Gamma_{ik}(x_m, p_m) e_i^{[j]} e_k^{[l]}. \quad (9)$$

Symbols $e_i^{[j]}$ in 9 denote the components of unit vectors $\mathbf{e}^{[j]}$. Vectors $\mathbf{e}^{[1]}$ and $\mathbf{e}^{[2]}$ are perpendicular to the third vector $\mathbf{e}^{[3]}$ chosen so that $\mathbf{e}^{[3]} = \mathbf{n}$. Here $\mathbf{n}$ is a unit vector specifying the direction of the first-order slowness vector $\mathbf{p}$. Vectors $\mathbf{e}^{[K]}$ can be chosen arbitrarily in the plane perpendicular to $\mathbf{n}$. Vector $\mathbf{e}^{[3]}$ can be determined from the second set of FORT equations 1. Along the common S-wave ray, vectors $\mathbf{e}^{[K]}$ can be computed as the vectorial base of the *wavefront orthonormal coordinate system*, see, e.g., Červený (2001):

$$\frac{de_i^{[K]}}{d\tau} = -(c^{[\mathscr{M}]})^2 (e_k^{[K]} \frac{dp_k}{d\tau}) p_i. \quad (10)$$

Elements of the matrix $\mathbf{M}(x_m, p_m)$, which appear in the "separation" term on the right-hand side of equation 6 read:

$$M_{KL}(x_m, p_m) = B_{KL}(x_m, p_m) - \frac{B_{K3}(x_m, p_m) B_{L3}(x_m, p_m)}{B_{33}(x_m, p_m) - 1}, \quad (11)$$

Quantities B_{ij} are again elements of the matrix $\mathbf{B}(x_m, p_m)$ given in equation 9.

Examples

In order to illustrate the accuracy of the approximate traveltime formulae 5-7, we consider the VSP configuration, which we used in our previous studies of FORT and FODRT for P waves, see Pšenčík and Farra (2005, 2007). The source and the borehole are situated in a vertical plane (x,z). The borehole is parallel to the z axis, the source is located on the surface at $z = 0$ km, at a distance of 1 km from the borehole. There are 29 three-component receivers in the borehole, distributed with a uniform step of 0.02 km, with receiver depths ranging from 0.01 to 0.57 km.

We consider three models, QI, QI2 and QI4, used by Klimeš and Bulant (2004) and Bulant and Klimeš (2008). The models are vertically inhomogeneous HTI media with constant vertical gradients of the elastic moduli. The axis of symmetry is rotated everywhere in the horizontal plane by 45^o from the vertical plane (x,z). The S-wave anisotropy defined as $(c_{S1} - c_{S2})/c_{average} \times 100\%$ ranges, from the horizontal to vertical direction, from 1% to 4%, from 4% to 7% and from 11% to 13% for the QI, QI2 and QI4 models, respectively. The matrices of the density-normalized elastic moduli can be found in the above references. The variations of the S-wave phase velocities in the (x,z) plane for all three models are shown in Figure 1. The left-hand plots correspond to $z = 0$ km, the right-hand plots to $z = 1$ km. Model QI is shown in the top, QI2 in the middle and QI4 in the bottom plot. Velocities are shown as functions of the angle of incidence. They vary from 0^0 (horizontal propagation) to 90^0 (vertical propagation). Although the formulae 5-7 can be used in arbitrary laterally inhomogeneous media, the models used here exhibit only vertical variations.

Figure 2 shows the relative traveltime differences for the QI4 model. The relative difference of traveltime τ is computed as

$$\frac{\tau_{APPR} - \tau_{EXACT}}{\tau_{EXACT}} \times 100\%. \quad (12)$$

In Figure 2, τ_{APPR} is the first-order traveltime $\tau^{[\mathscr{M}]}$ computed along the common ray. The time τ_{EXACT} is computed along rays of S1 and S2 waves, by the ray tracer for anisotropic media – a modified program package ANRAY (Gajewski and Pšenčík, 1990). Blue corresponds to the faster S1 wave, red to the slower S2 wave. We can see that the deviations of $\tau^{[\mathscr{M}]}$ from the exact traveltimes of the faster S1 wave is between 2-3% while the deviation of $\tau^{[\mathscr{M}]}$ from the exact traveltime of the S2 wave reaches 9%.

The above deviations are strongly reduced if we correct $\tau^{[\mathscr{M}]}$ by the perturbation terms in equation 6. The results are shown in Figure 3, this time for all three models. Again, blue denotes the faster S1 wave, red the slower S2 wave. We can see that the proposed corrections in equation 6 yield approximate traveltimes τ_{S1} and τ_{S2}, whose relative errors are much less than 1% for all three models. The approximate traveltimes are in all cases less than standard ray-theory traveltimes, which confirms a similar observation of Farra & Pšenčík (2009). In case of weak anisotropy (model QI and partially QI2), the relative errors are so small that they are comparable with errors of the two-point ray tracing procedure. This leads to the chaotic behavior of errors. In model QI, the relative errors of traveltimes of both waves are about 0.02%. For QI2 and QI4 models, the errors of the faster S1 wave are less than 0.1 and 0.4%, respectively. The errors corresponding to S2 waves are slightly larger, around 0.1 and 0.5%.

Conclusions

Recent developments in the theory of first-order ray tracing for simulation of coupled S waves in inhomogeneous weakly anisotropic media make it possible to estimate specific traveltimes of the S-wave events. Knowledge of such specific traveltimes is of importance in migration and tomography applications. In this contribution we have tested the new formulae in three models possessing TI anisotropy. The results are highly satisfactory and indicate that the theory can be applied also beyond weak anisotropy.

Acknowledgements

This contribution is dedicated to the memory of Michael Schoenberg. A substantial part of the work was done during IP's stay

in Paris at the invitation of the IPGP. We acknowledge support by the Consortium Project "Seismic waves in complex 3-D structures" (SW3D), the Research Project 205/08/0332 of the Grant Agency of the Czech Republic, and the Research Council of Norway via NORSAR's SIP project 181688/I30.

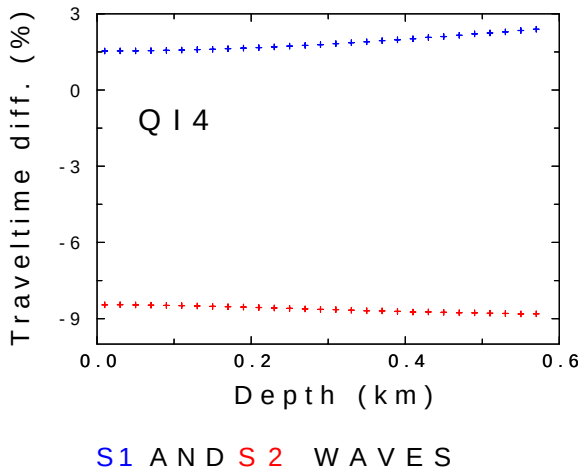

Figure 2: Model QI4. The relative differences of the first-order traveltime $\tau^{[\mathscr{M}]}$ and the exact traveltimes of the faster S1 (blue) and the slower S2 (red) waves.

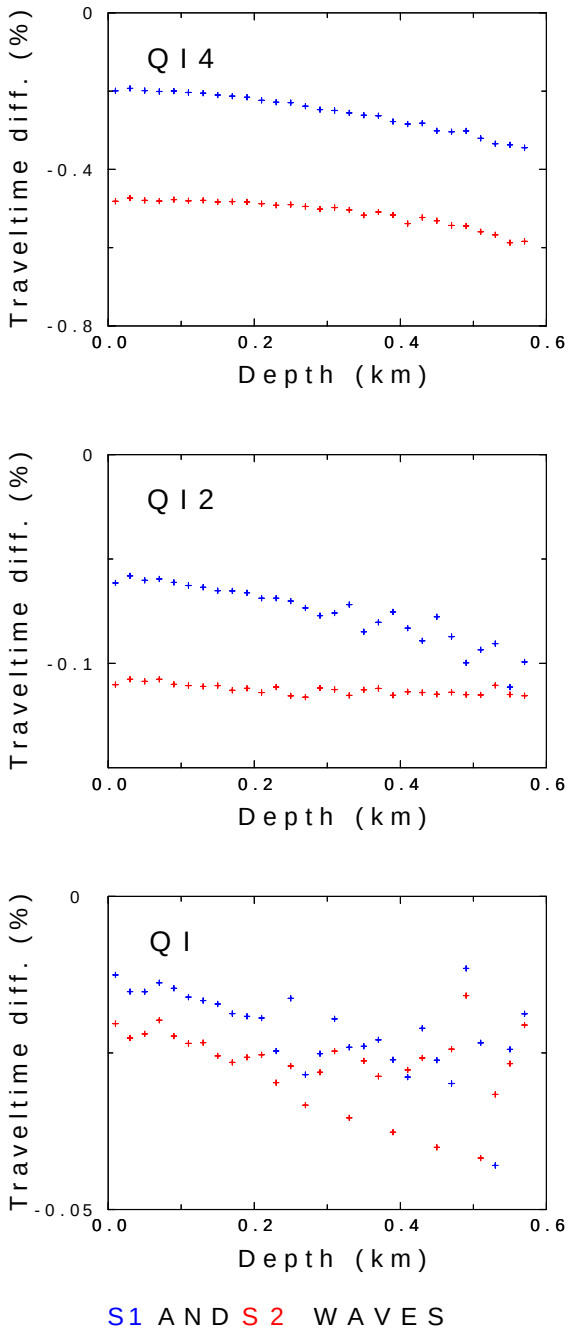

Figure 3: Models QI, (bottom), QI2 (middle) and QI4 (top). The relative differences of the approximate traveltimes τ_{S1} (blue) and τ_{S2} (red) and the exact traveltimes of the faster S1 (blue) and the slower S2 (red) waves.

References

Bakker, P., 2002. Coupled anisotropic shear-wave ray tracing in situations where associated slowness sheets are almost tangent, *Pure Appl. Geophys.*, **159**, 1403–1417.

Bulant, P. & Klimeš, L., 2002. Numerical algorithm of the coupling ray theory in weakly anisotropic media, *Pure Appl. Geophys.*, **159**, 1419–1435.

Bulant, P. & Klimeš, L., 2008. Numerical comparison of the isotropic- common-ray and anisotropic-common-ray approximations of the coupling ray theory, *Geophys. J. Int.*, **175**, 357–374.

Červený, V., 2001. *Seismic Ray Theory*, Cambridge Univ. Press, Cambridge.

Coates, R.T. & Chapman, C.H., 1990. Quasi–shear wave coupling in weakly anisotropic 3-D media, *Geophys. J. Int.*, **103**, 301–320.

Farra, V. & Pšenčík, I., 2008. First-order ray computations of coupled S waves in inhomogeneous weakly anisotropic media, *Geophys. J. Int.*, **173**, 979–989.

Farra, V. & Pšenčík, I., 2009. Coupled S waves in inhomogeneous weakly anisotropic media using first-order ray tracing: Geophysical Journal International, submitted.

Gajewski, D., & Pšenčík, I., 1990. Vertical seismic profile synthetics by dynamic ray tracing in laterally varying layered anisotropic structures, *J. Geophys. Res.*, **95**, 11301–11315.

Klimeš, L., 2006. Common-ray tracing and dynamic ray tracing for S waves in a smooth elastic anisotropic medium, *Stud. Geophys. Geod.*, **50**, 449–461.

Klimeš, L. & Bulant, P., 2004. Errors due to the common ray approximations of the coupling ray theory, *Stud. Geophys. Geod.*, **48**, 117–142.

Pšenčík, I., & Farra, V., 2005. First-order ray tracing for qP waves in inhomogeneous weakly anisotropic media, *Geophysics*, **70**, D65–D75.

Pšenčík, I. & Farra,V., 2007. First-order P-wave ray synthetic seismograms in inhomogeneous weakly anisotropic media. *Geophys. J. Int.*, **170**, 1243–1252.